pD8

EFFECT OF SUBSTRATES ON THE STRUCTURAL AND MORPHOLOGY OF TiO_2 THIN FILMS GROWN BY Nd-YAG LASER ANNEALING

Faouzi HANINI [1], Yacine BOUACHIBA [1], Fouad KERMICHE [1], Adel TAABOUCHE [1], Abderrahmane BOUABELLOU [1], Tahar KERDJA [2], Mohamed BOUAFIA [3] and Saad AMARA [3]

[1]*Laboratoire Couches Minces – Interfaces, Université Mentouri – Constantine, 25000, Algérie*
[2]*Centre de Développement des Techniques Avancées, Baba-Hassen, 16000 Alger, Algérie*
[3]*Département d'Optique et de Mécanique de Précision, Université Ferhat Abbès – Sétif, Sétif, Algérie*
E-mail: haninifaouzi@gmail.com

ABSTRACT: Thin films of titanium oxide (TiO_2), 350–400 nm thick, were prepared by pulsed laser deposition (PLD) on glass/MgO-poly/Si-poly/Si(111)/Si(100) at a substrate temperature of 450°C. The used source was a Nd:YAG laser (λ = 266 nm, ν = 5 Hz, Φ = 2 J/cm^2 and τ = 8 ns pulse duration). The effects of substrates on the crystalline structure and morphology of TiO_2 thin films have been investigated. X-ray diffraction reveals that the material deposited is polycrystalline titanium oxide having primitive tetragonal anatase-type structure. The lattice parameters, grain size, microstrain and dislocation densities were calculated and correlated with the substrate material and its orientation. The surface morphologies of the TiO_2 thin films deposed on different substrates were evaluated by atomic force microscopy (AFM). The optical gap of TiO_2 thin film was determined using the optical transmission spectrum and the optical band obtained is equal to 3.24 eV.

KEYWORDS: TiO_2, Nd:YAG laser, substrate, structural analysis, morphology, optical transmittance

1. Introduction

TiO_2 thin films have attracted a great deal of attention, due to their excellent physicochemical properties, such as crystallite structure, particle size, specific surface area, porosity and thermal stability. They have many advanced functions in dye-sensitized solar cell [1], gas sensors [2], photocatalysts [3], waveguiding [4], antireflective coatings [5], dielectric [6], etc. Titanium dioxide (TiO_2) belongs to the family of transition metal oxides [7]. In nature, TiO_2 is known to occur in the structures of rutile, anatase, and brookite (brookite is a minority product of most synthesis) [8]. A fourth polymorph, having the α-PhO_2 structure (orthorhombic), has recently been synthesized under high-pressure [9]. The structures of rutile, anatase and brookite can be discussed in terms of (TiO_2^{6-}) octahedrals are interconnected differently for each phase, leading to different structures and symmetries [7]. Rutile is a tetragonal with lattice of a = 4.594 Å, c = 2.958 Å. Anatase TiO2 is a tetragonal with lattice of a = 3.785 Å, c = 9.514 Å, and with optical band gap of 3.2 eV at room temperature. Brookite is an orthorhombic with lattice of a = 9.184 Å, b = 5.447 Å, c = 5.145 Å [7, 10]. TiO_2 thin films have been synthesized by different techniques such as sol–gel [11], ultrasonic spray pyrolysis [12], cathodic electrodeposition [13], layer-by-layer (LBL) self-assembly [14], atmospheric pressure chemical vapour deposition [15], reactive magnetron sputtering [16] or pulsed laser deposition (PLD) [17]. It is known that PLD has numerous advantages over the classical deposition methods. The thin films obtained previously by PLD were either amorphous [18], sub-stoichiometric [19] or contained a mixture of rutile and anatase phases [20]. Moreover, the synthesis by PLD of brookite rich

TiO_2 films was reported along with anatase and a small amount of rutile [21]. Other authors found that the crystalline phase of the films is also influenced by the ambient oxygen pressure [22] as well as the substrate material and its orientation [23].
In this paper, we report the successful growth of pure anatase phase TiO_2 on different substrates by Nd:YAG PLD technique. The aim of this study is to investigate effect of substrate type on the TiO_2 thin films. The structural, optical properties and morphology of the TiO_2 films were characterized.

2. Experimental

A Nd: YAG laser (λ = 266 nm, ν = 5 Hz and τ = 8 ns pulse duration) with a fluence of Φ = 2 J/cm^2 was focused on a sintered TiO_2 ceramic target. We used a stainless steel chamber that can be evacuated to a base pressure of 1x10^{-5} Torr by means of a turbo-molecular pump. A glass, MgO-poly, Si-poly and Si(111) were used as substrates for film deposition. The distance between the substrate and target was kept fixed at 50 mm and the substrate temperature is maintained at 450°C under an oxygen of pressure of 2 mTorr. The beam laser was incident on the rotating target at an angle of 45° with respect to the target normal. The ceramic target (20 mm×5 mm) was prepared by palletizing special grade TiO_2 powder using a uniaxial press at 15 MPa, followed by sintering at 1000 °C for 2 h in air.
The crystal structure of the synthesized TiO_2 films was characterized by Grazing Incidence X-ray diffraction (GIXRD) Bruker-AXS D8 diffractometer using CuKα radiation (λ = 0.154056 nm) and operated in $\theta/2\theta$ configuration. Atomic force microscopy (AFM) (Pacific Nanotechnology) operating in contact mode was used for the observation of surface morphology for TiO_2 films deposited on different substrates in a region of 2.34×2.34 µm^2 area. The optical properties of the TiO_2 thin films were characterized by UV-VIS spectrometer Shimadzu (UV-3101 PC) in the wavelength range 300-900 nm.

3. Results and discussion

3.1. X-ray diffraction analysis

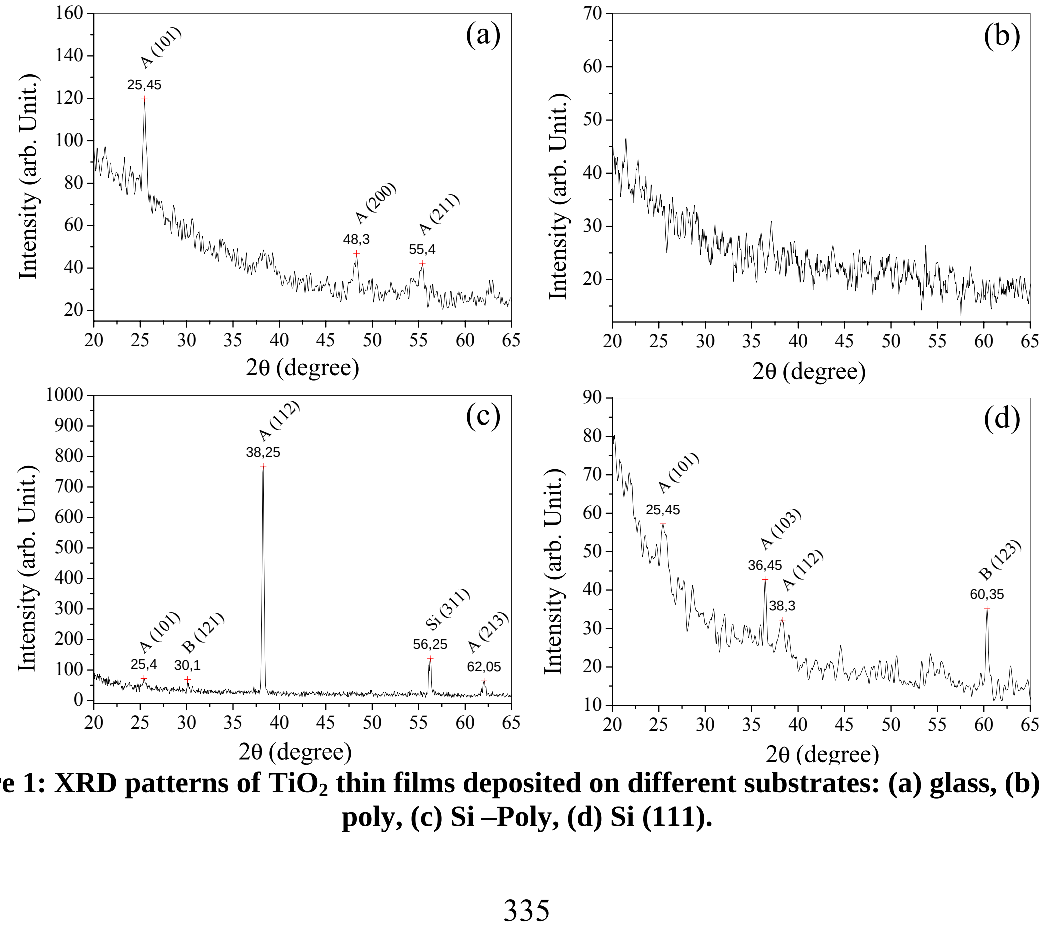

Figure 1: XRD patterns of TiO_2 thin films deposited on different substrates: (a) glass, (b) MgO-poly, (c) Si –Poly, (d) Si (111).

The XRD patterns of TiO_2 at 450°C onto different substrates are shown in Fig. 1. It shown that material deposited on glasse and Si-poly substrates is TiO_2 polycrystalline in nature. A matching of the observed and the standard (*hkl*) plans confirms that the deposited films are of TiO_2 having primitive tetragonal anatase type structure [24]. The films deposited on MgO-poly substrate were amorphous in nature. On the other hand, some peaks can be observed in the films deposited on Si-poly and Si (111) substrates. The peaks observed at 30.01 and 60.35° correspond to brookite (121) and (123) respectively, were also present in the XRD patterns (Fig. 1).

3.2. Study of lattice constant, grain size, microstrains and dislocation density

The constant 'a', 'b' & 'c', for the tetragonal phase anatase-type structure determined by the relation:

$$d_{hkl} = \frac{\lambda}{2\sin\theta} = \frac{ac}{\sqrt{a^2l^2 + c^2\left(h^2 + k^2\right)}} \qquad (1)$$

Where 'd_{hkl}' is the interplaner distance and (*hkl*) are miller indices, respectively. The lattice constant '*a*', 'b' & '*c*' calculated and are given in table 1.

The average grain size of TiO_2 thin films were estimated for all the observed planes by using the Scherer's formula [25].

$$D_{(nm)} = \frac{k\lambda}{\beta\cos\theta} \qquad (2)$$

where '*k*' varies from 0.89 to 1.39. But in most of the cases it is closer to 1. Hence for grain size calculation it is taken as one, 'λ' is wavelength of X-ray, 'β' is the full-width at half of the peak maximum in radians and 'θ' is Bragg's angle. The variation of the grain size of TiO_2 thin films is shown in Table 1.

Table 1: Structural parameters of Nd-YAG laser deposited titanium oxide thin films.

TiO_2 film	2θ (°)	d_{hkl} (Å)	(*hkl*)	a (Å)	c (Å)	Avg. D (nm)	ρ_D x 10^{14} linces/m^2	ε x 10^{-3}
Glass	25.45	3.497	101	3.764	9.430	21.410	2.18	4.45
	48.30	1.882	200					
	55.40	1.657	211					
Mgo-Poly	Amorphous nature							
Si-Poly	25.40	3.503	101	3.770	9.470	9.646	10.07	6.51
	38.25	2.351	112					
	62.05	1.494	213					
Si(111)	25.45	3.496	101	3.741	9.808	28.253	1.25	3.42
	36.45	2.462	103					
	38.30	2.348	112					

The FWHM (β) and residual microstrain can be related according to the following equation [26]

$$\beta\, cos\,\theta = \frac{k\lambda}{D} + 4\varepsilon\, sin\,\theta \qquad (3)$$

The strain ε was estimated from the slope of the plot β *cos*θ vs. *sin*θ; the calculated values are given in Table1. The decrease in microstrain indicates a decrease in lattice imperfections. In our case, dislocation density (ρ_D) was determined using the relation [26] as (Tabl.1)

$$\rho_D = \frac{1}{D^2} \qquad (4)$$

3.3. Morphological characterization

Fig. 4 shows AFM topographies of the TiO_2thin films deposited on glass/MgO-poly/Si-poly/Si(111) substrates. The average mean roughness (Rms) of the surfaces is calculated for a 5.51μm^2 square scan area. It is found that the mean roughness significantly decreases from 22 to 4 nm of TiO_2 films deposited onto Si-poly, Si(111), glass, and MgO substrates respectively. However, these differences in average mean roughness have a significant influence on optical properties of the films considered in this study. These results, together with the XRD analysis, clearly indicate that the crystallinity is influenced by the substrates.

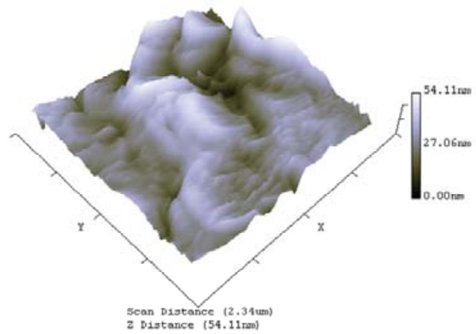

(a) Rms = 6.0105 nm

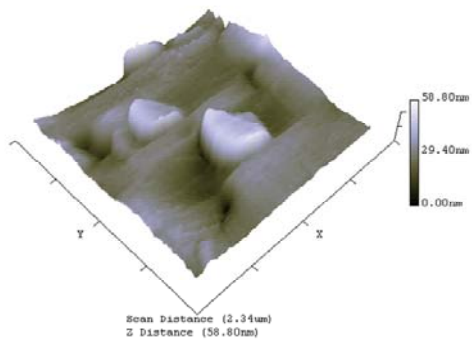

(b) Rms = 4.5712 nm

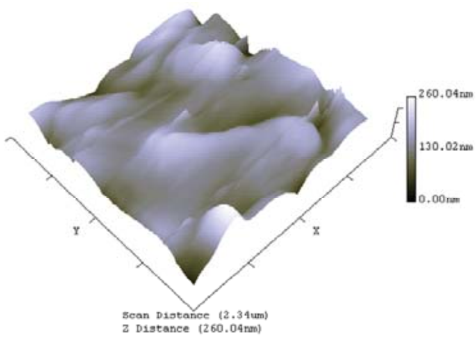

(c) Rms = 22.0408 nm

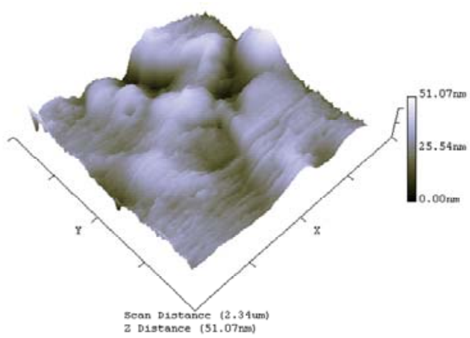

(d) Rms = 5.2124 nm

Figure 3: AFM images of TiO_2 thin films deposited on glass (a), poly -MgO (b), Poly-Si (c) and (111)-Si (d) substrates. The root mean squares (Rms) are also indicated in the figure.

3.4. Optical characterization

Fig. 4 shows the transmission spectra of TiO_2 thin film deposited onto glass substrates in the wavelengths range of 200-900 nm. All the measurements are realized at room temperature.

As can be seen, the average optical transmittance of the samples in the visible range is amount 70%. In addition, it is important to notice that the films have a suitable thickness (~ 300 nm), leading to a good optical quality of the produced TiO_2 materials which is in good agreement with the literature reports [12, 13].

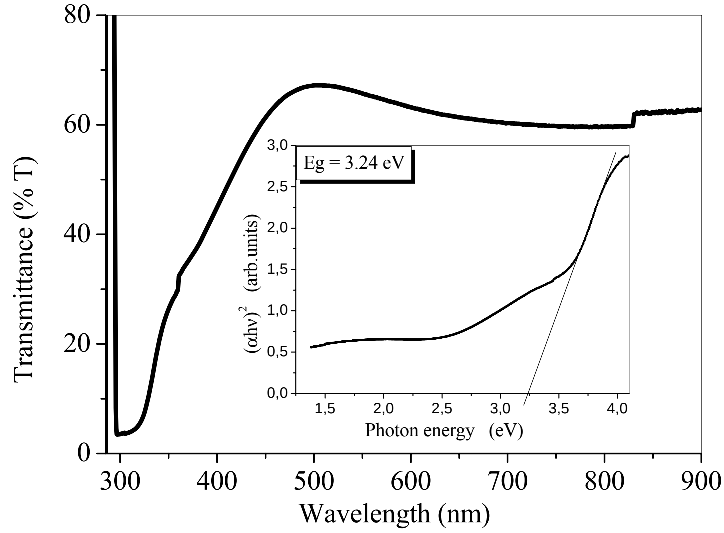

Figure 4: Optical Transmittance spectra of TiO_2 thin films deposited on glass substrate by PLD (The Inset shows plot of $(\alpha h\nu)^2$ versus $h\nu$).

The band gap E_g was calculated using the Tauc equation [25]:

$$\alpha h\nu = B(h\nu - Eg)^n \quad (6)$$

where $h\nu$ is the photons energy; E_g is the optical band gap corresponding to transitions indicated by the value of n. In particular, n is 1/2, 3/2, 2 and 3 for direct allowed, direct forbidden, indirect allowed and indirect forbidden transitions, respectively. The factor B depends on the transition probability and can be taken constant within the investigated optical frequency range. The absorption coefficient α could be calculated from the following equation [25]:

$$\alpha = \frac{\ln\left(\frac{1}{T}\right)}{d} \quad (7)$$

where T is the transmittance and d is the thickness of the film. The plot of the graph $(\alpha h\nu)^2$ vs $h\nu$ (see inset Fig. 4) is accomplished using formula (7). The band gap value of the produced TiO_2 films, determined by the optical method, is obtained by extrapolating the linear portion of this graph to $(\alpha h\nu)^2 = 0$. As can be seen from the Fig. 4, E_g is equal to 3.24 eV.

4. Conclusion

Properties of TiO_2 thin films grown by Nd:YAG laser onto different substrates including glass, MgO-poly, Si-poly and Si(111) were investigated. It was observed that the substrate nature was a strong factor influencing the properties of TiO_2 films. The produced TiO_2 thin films are polycrystalline with a tetragonal pure anatase–type structure. The values of grain sizes vary from 9 to 28 nm and the mean roughness increases up to 6-22 nm in the case of the Si-poly substrate. The transmission of the TiO_2 films is about 70% and the deduced value of their optical band gap is 3.24 eV.

References

[1] Antonio Otávio T. Patrocínio, Eucler B. Paniago, Roberto M. Paniago, Neyde Y. Murakami Iha, *Appl. Surf. Sci* **254,** 1874–1879 (2008).

[2] Ibrahim A. Al-Homoudi, J.S. Thakur, R. Naik, G.W. Auner, G. Newaz, *Appl. Surf. Sci* **253**, 8607–8614 (2007).

[3] M.R. Hoffmann, S.T. Martin,W. Choi, D.W. Bahnemann, *Chem. Rev.* **95**, 69–96 (1995).

[4] R. Mechiakh, F. Meriche, R. Kremer, R. Bensaha, B. Boudine, A. Boudrioua , *Optical Materials* **30**, 645–651 (2007).

[5] Sang-Hun Jeong, Jae-Keun Kim, Bong-Soo Kim, Seok-Ho Shim, Byung-Teak Lee, *Vacuum* **76**, 507–515 (2004).
[6] Wenli Yang, Colin A. Wolden, *Thin Solid Films* **515**, 1708–1713 (2006).
[7] O. Carp, C.L. Huisman, A. Reller, *Progress in Solid State Chemistry* **32**, 33–177 (2004).
[8] Y.F. Chen, C.Y. Lee, M.Y. Yeng, H.T. Chiu, *Mater. Chem. Phys.* **81**, 39–44 (2003).
[9] D.W. Meng, X.L. Wu, F. Sun, L.W. Huang, F. Liu, Y.J. Han , J.P. Zheng, X. Meng, R. Mason**,** *Micron* **39**, 280–286 (2008).
[10] C.-K. Jung, B.-C. Kang, H.-Y. Chae, Y.-S. Kim, M.-K. Seo, S.-K. Kim, S.-B. Lee, J.-H. Boo, Y.-J. Moon, J.-Y. Lee, *Journal of Crystal Growth* **235**, 450–456 (2002)
[11] R. Mechiakh, F. Meriche, R. Kremer, R. Bensaha, B. Boudine, A. Boudrioua, *Optical Materials* 30, 645–651 (2007).
[12] V. Jokanovic, A.M. Spasic, D. Uskokovic, *Journal of Colloid and Interface Science* **278**, 342–352 (2004).
[13] S. Karuppuchamy, J-M. Jeong, D.P. Amalnerkar, H. Minoura, *Vacuum* **80**, 494–498 (2006).
[14] Jin-Ho Kim, Shiro Fujita, Seimei Shiratori, *Thin Solid Films* **499**, 83–89 (2006).
[15] Charles W.H. Dunnill, Zoie A. Aiken, Jonathan Pratten, Michael Wilson, David J. Morgan, Ivan P. Parkin, *Journal of Photochemistry and Photobiology A: Chemistry* **207**, 244–253 (2009).
[16] Makiko Yamagishi, Shna Kuriki, P. K. Song, Yuzo Shigesato, *Thin Solid Films* **442**, 227–231 (2003).
[17] S. Yamamoto, T. Sumita, T. Yamaki, A. Miyashita, H. Naramoto, *Journal of Crystal Growth* **237–239**, 569–573 (2002).
[18] N. Lobstein, E. Millon, A. Hachimi, J.F. Muller, M. Alnot, J.L. Ehrhardt, Appl. Surf. Sci. **89**, 307-321 (1995).
[19] H.K. Ardakani, *Thin Solid Films* **248**, 234-239 (1994).
[20] A. Suisalu, J. Aarik, H. Mandar, I. Sildos, *Thin Solid Films* **336**, 295-298 (1998).
[21] M.P. Moret, R. Zallen, D.P. Vijay, S.B. Desu, *Thin Solid Films* **366**, 8-10 (2000).
[22] D.G. Syarif, A. Miyashita, T. Yamaki, T. Sumita, Y. Choi, H. Itoh, *Appl. Surf. Sci.* **193**, 287-292 (2002).
[23] S. Yamamoto, T. Sumita, A. Sugiharuto, H. Miyashita, Naramoto, *Thin Solid Films* **401**, 88-93 (2001).
[24] Natl. bur. Stand. (U.S.) 25, 7, 82 (1969).
[25] Bin Zhou, Meghan Schulz, H.Y. Lin, S. Ismat Shah, Jiuhui Qu, C.P. Huang, *Applied Catalysis B: Environmental* **92**, 41–49 (2009).
[26] B. D. Cullity, Elements of X-ray Diffraction, A. W. Pub. Comp. Inc., (1978).